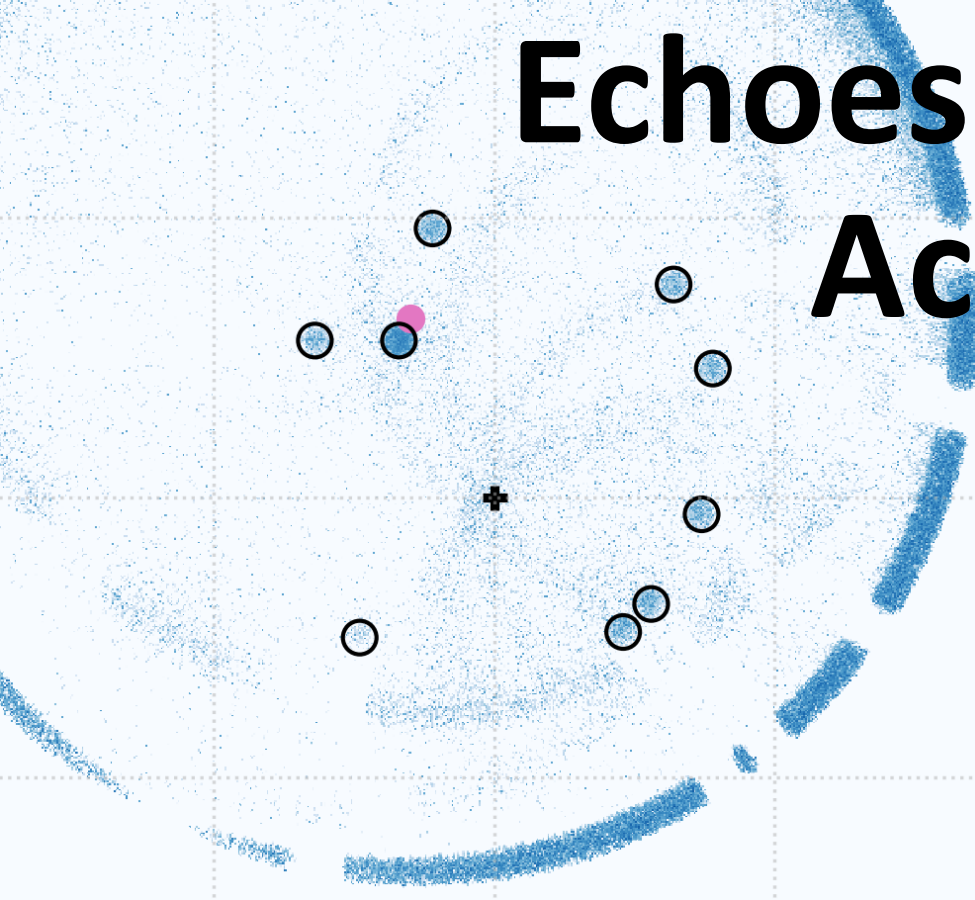


Echoes from Cen A's Active Past



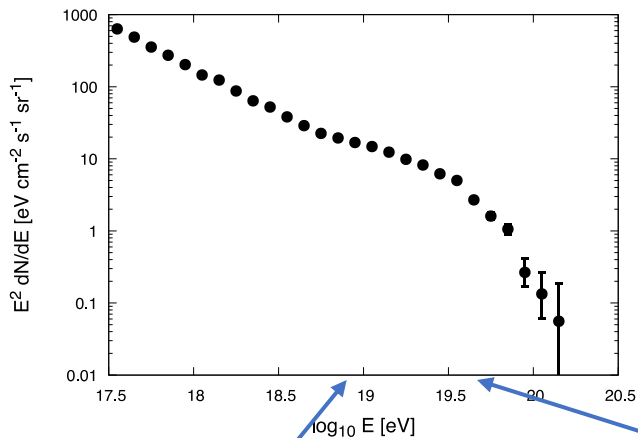
Work done in collaboration with:
James Matthews (University of Oxford)
and
Tony Bell (University of Oxford)

Taylor et al. MNRAS 524 (2023)

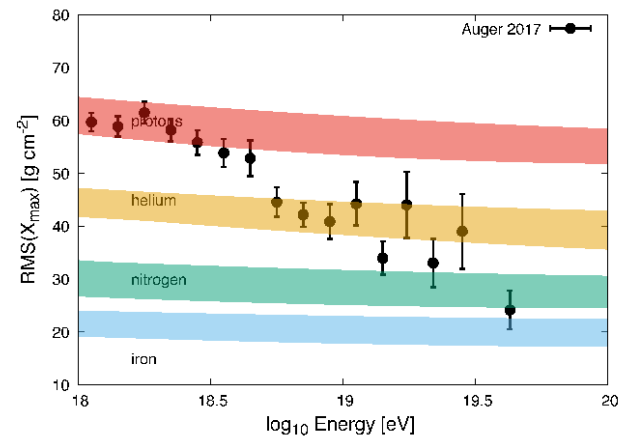
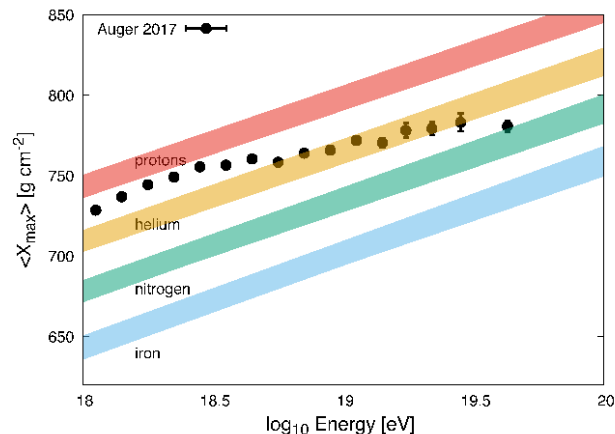
Building on the results of Bell et al. MNRAS 448 (2022)

UHECR: The Observational Status

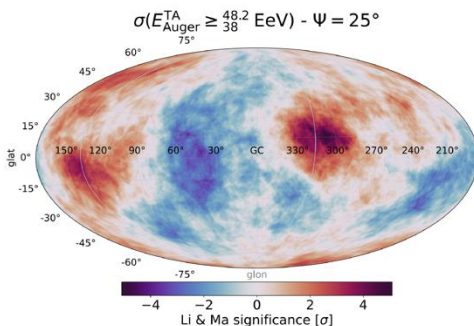
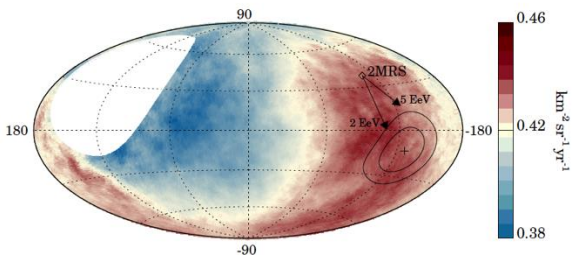
Spectrum



Composition



Anisotropy



Pierre Auger Collaboration. Science 357 (2018)

Caccianiga et al. for the Auger & TA Collaborations. PoS (ICRC2023) 521

Pierre Auger Collaboration. ApJ. 935 (2022)

UHECR: The Challenge of Theoretical Interpretation

Global fits to the spectrum and composition data, assuming a continuous distribution of sources, motivate a **hard source spectrum**

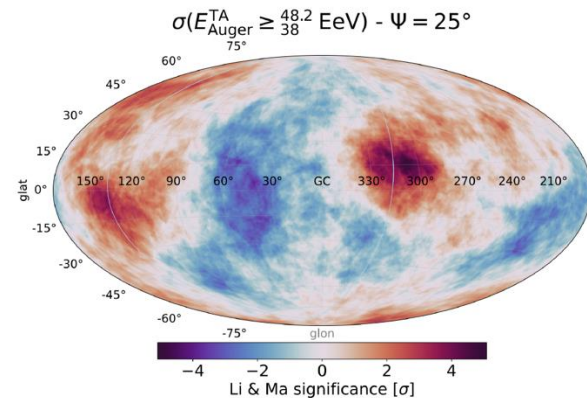
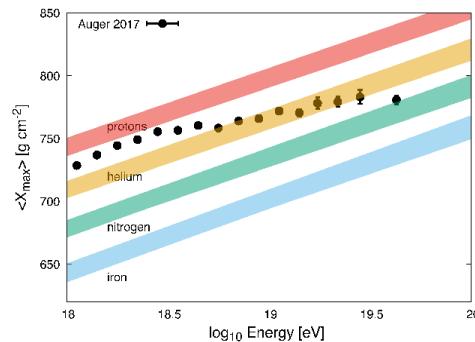
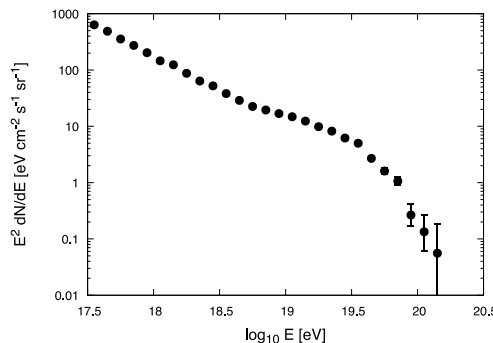
Taylor, PRD 92 (2015) 6

PAO, JCAP 04 (2017) 038

Such a solution appears “unstable”, with the addition of a small range of maximum rigidity cutoff for the sources (ie. non-identical source spectra) being unable to maintain a good fit, requiring instead **near-identical sources**

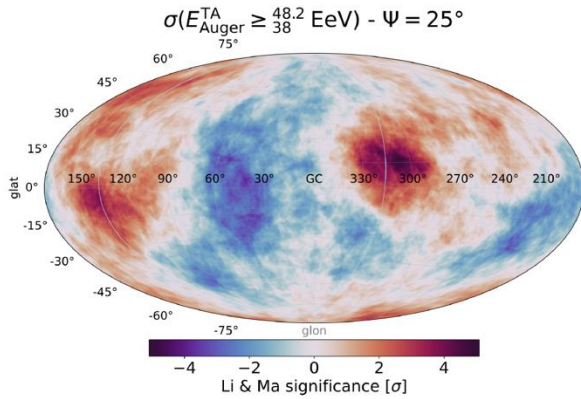
Ehlert, PRD 107 (2023) 10

A **single local source** can alleviate both of these above listed problems. However, this idea is criticized as being incompatible with the observed UHECR anisotropy. It is this criticism which I will here focus on.

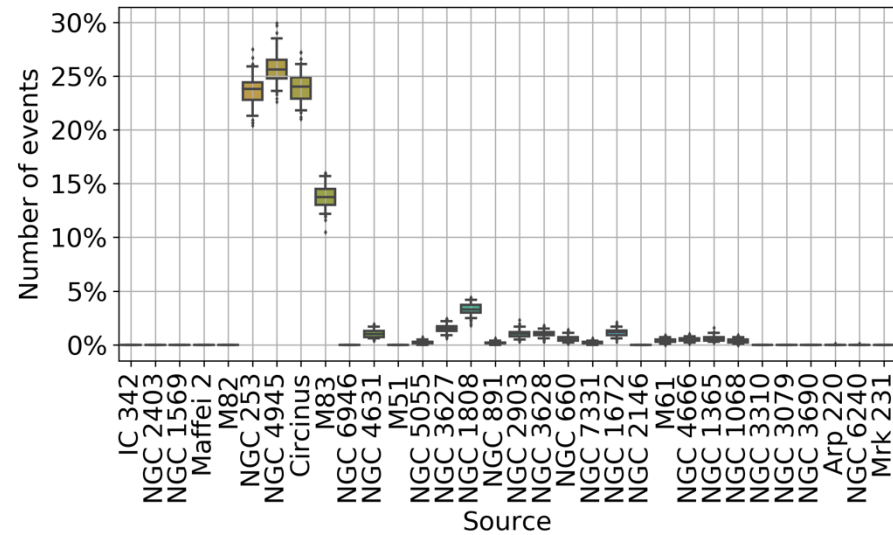


Our Local Extragalactic Neighbourhood

The local (<10 Mpc) extragalactic objects are structured, sitting in a roughly circular disk shape around the Milky Way

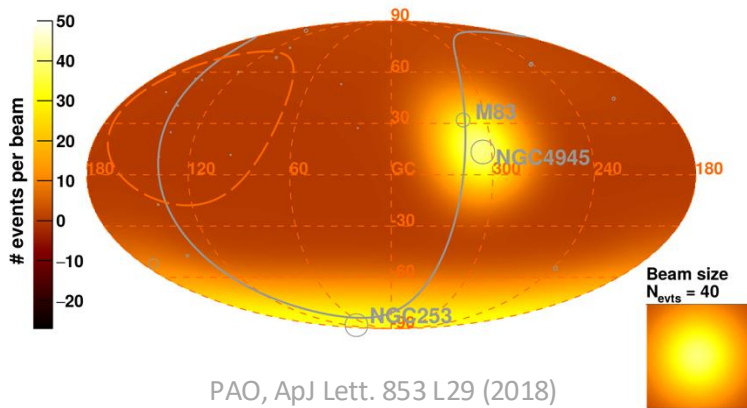


van Vliet MNRAS 510 (2021) **Correlation Drivers**



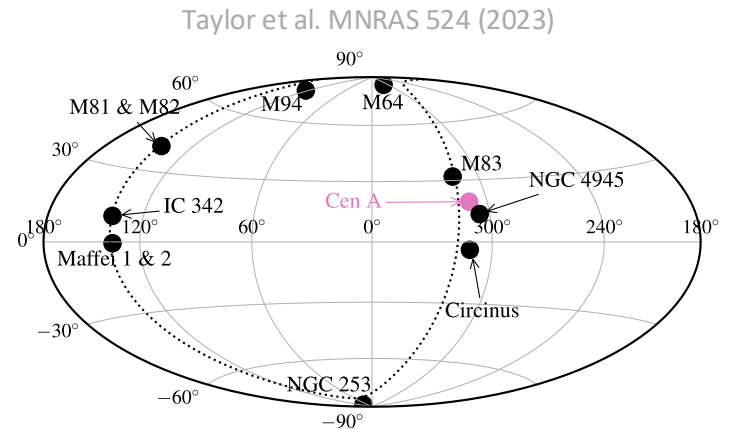
Caccianiga et al. for the Auger and TA Collaborations. PoS (ICRC2023) 521

Model Excess Map - Starburst galaxies - $E > 39$ EeV



PAO, ApJ Lett. 853 L29 (2018)

Local Extragalactic Object Skymap



Taylor et al. MNRAS 524 (2023)

Andrew Taylor

Local Extragalactic Structure

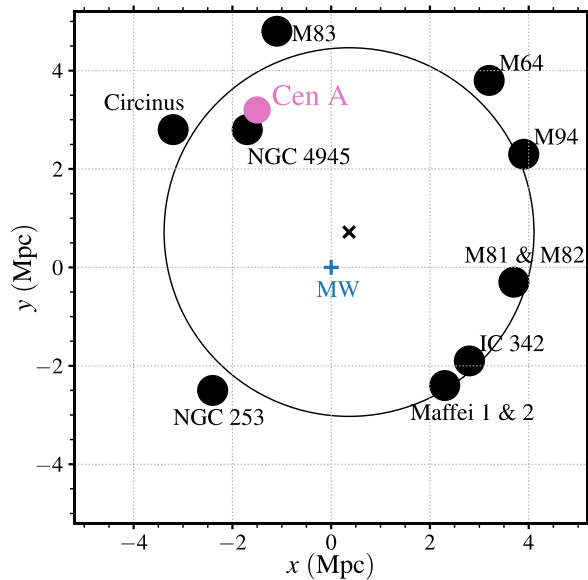
The Council of Giants

Cen A is unique within the council of giant structure are being the only object showing a kinetic luminosity capable of giving rise to multi EeV acceleration

Lovelace et al. (1976)

$$E_{\max} \lesssim \frac{Z}{\eta} (\beta L_{\text{KE}} \alpha \hbar)^{1/2} \approx 10 \frac{Z}{\eta} \left(\frac{\beta L_{\text{KE}}}{3 \times 10^{43} \text{ erg s}^{-1}} \right)^{1/2} \text{ EeV}$$

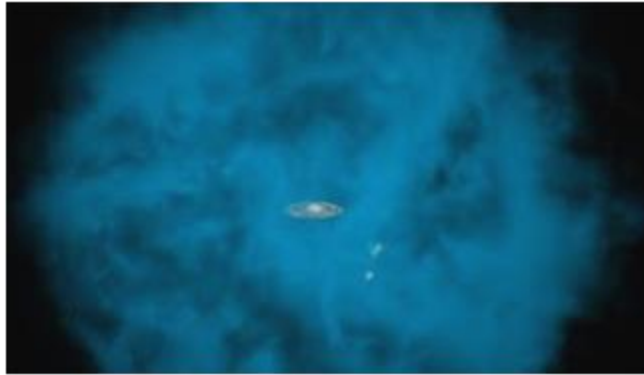
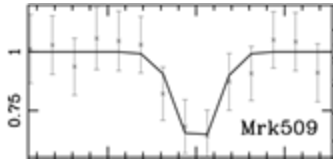
Local Extragalactic Objects in Local Sheet Coordinates



Large Thermal Pressure in Galactic Haloes

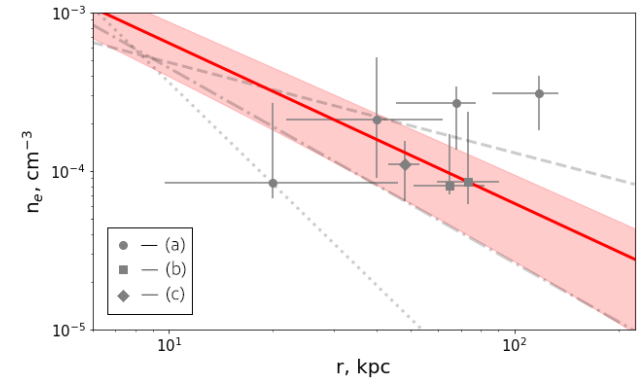
X-ray observations of bright AGN indicate the presence of a hot local absorber.

Gupta ApJ, 756 (2012)



More recently, the ram pressure stripping of satellite galaxies + emission from the hot absorber have been collectively used to probe the halo gas density.

Faerman ApJ 835 (2017), Martynenko MNRAS, 511 (2022)



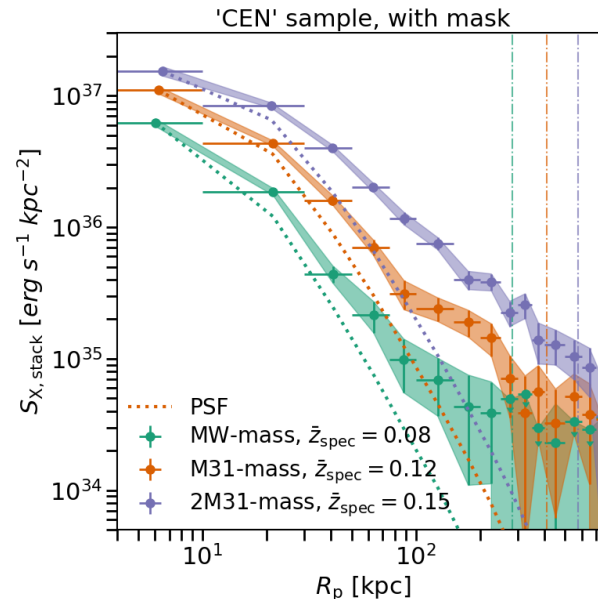
Bregman et al. ApJ 928 (2022)

Zhang et al. for the eRosita collaboration- A&A (2024)

$$\mathbf{n} = \mathbf{n}_0 \left[1 + \left(\frac{\mathbf{r}}{\mathbf{r}_c} \right)^2 \right]^{-\frac{2}{\beta}}$$

$$\beta \approx \mathbf{0.4} \pm \mathbf{0.1}$$

DESY.



Faerman ApJ, 893 (2020)

$$\mathbf{B(100\ kpc)} \approx \mathbf{0.2\ \mu G}$$

Heesen A&A, 670 (2023)

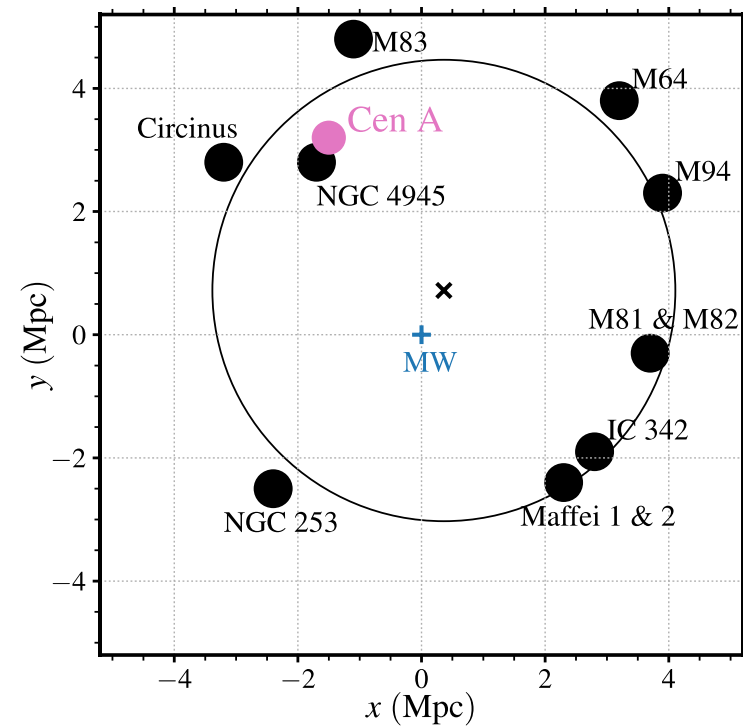
$$\mathbf{r_L(10\ EV)} = \mathbf{50\ kpc}$$

Simulation Setup

- Particles initially fill 300 kpc region surrounding Cen A (isotropic momentum distribution)
- Large angle particle scattering occurs within the virial region (< 300 kpc) of all members of the Council of Giant system
- Outside the virial radii of these galaxies the particle propagation is treated as ballistic
- A fundamental parameter of problem-optical depth of scattering regions

$$\tau = \frac{\mathbf{r}_{\text{vir}}}{\mathbf{l}_{\text{sc}}}$$

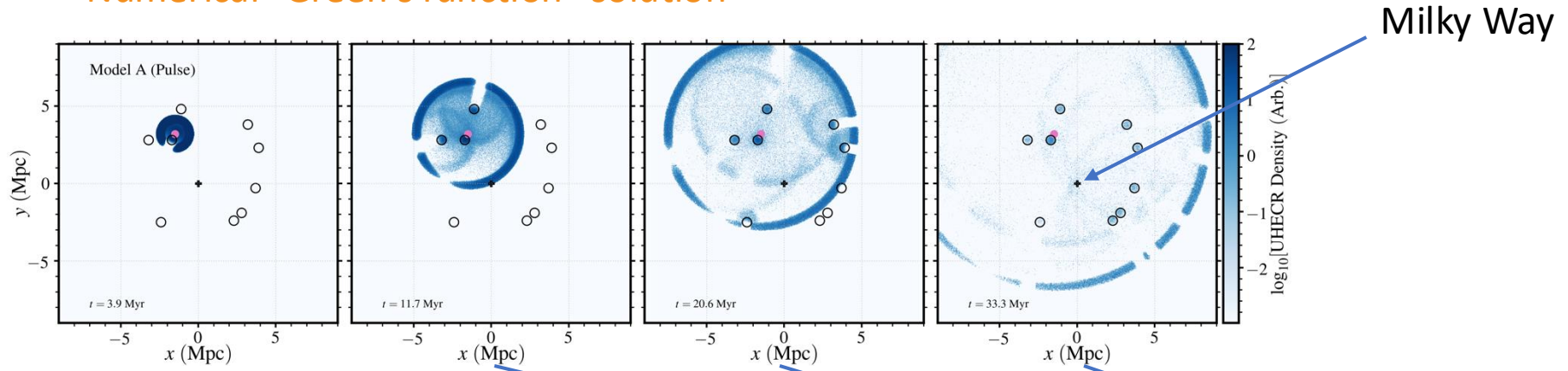
- Echo signal results are rather insensitive to optical depth of scattering regions, provided $\tau > 1$



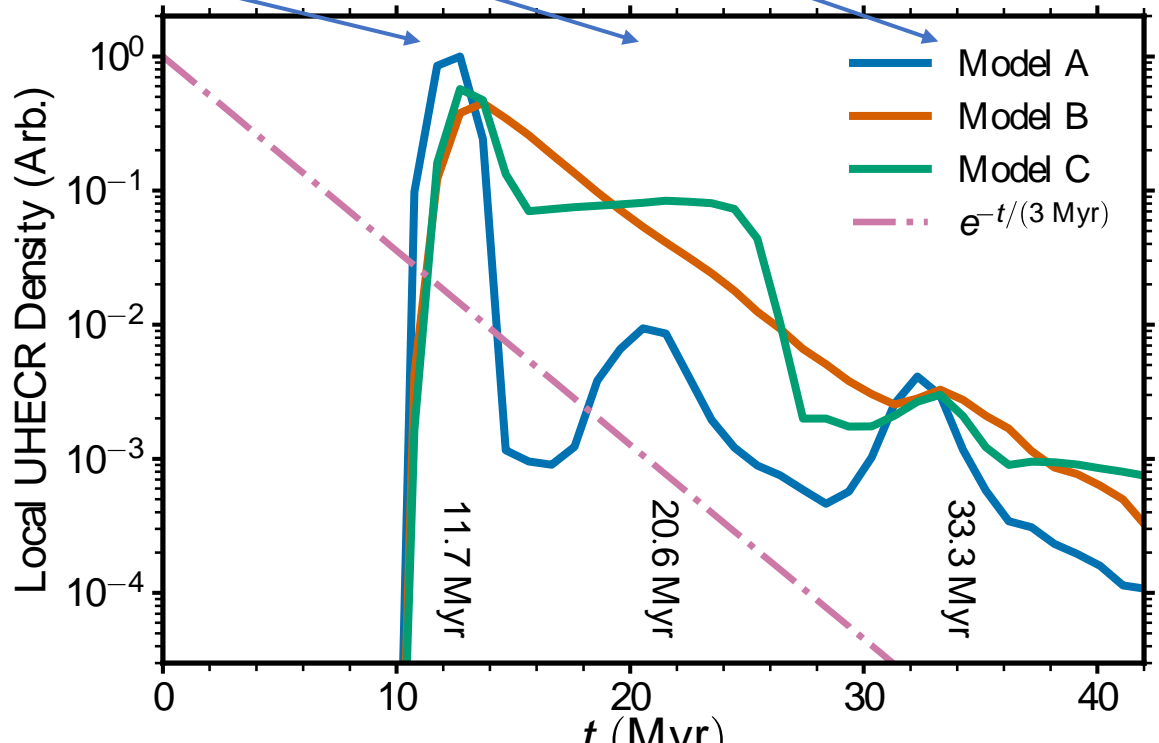
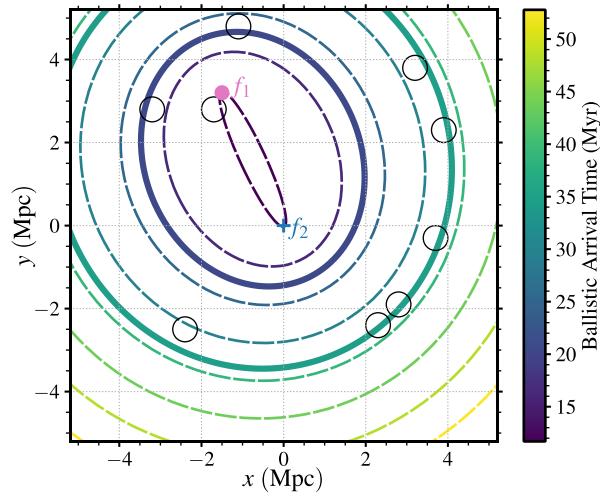
- Only He and Fe injected into the system (fragile and robust species compared to crossing time of system)
- Particles photo-disintegrate en-route in extragalactic radiation fields
- 30 EeV particles being focused on
- Deflections from MW magnetized halo intentionally left out

Echo Waves

Numerical "Green's function" solution

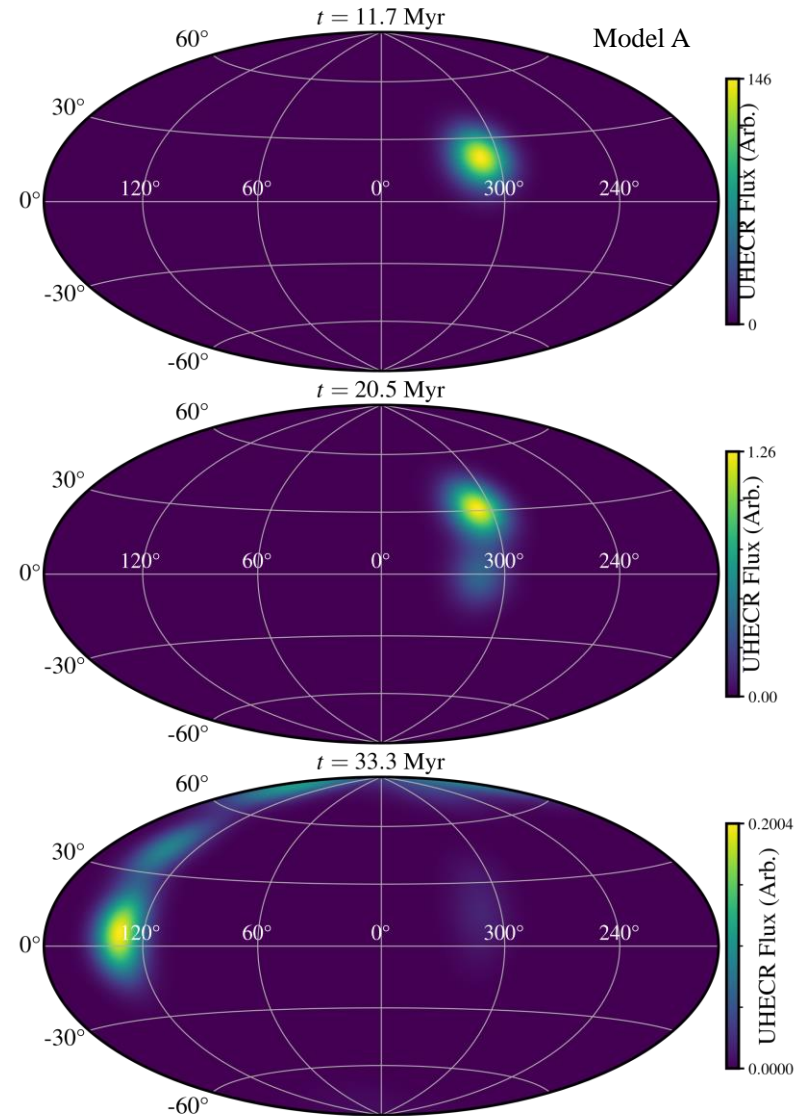
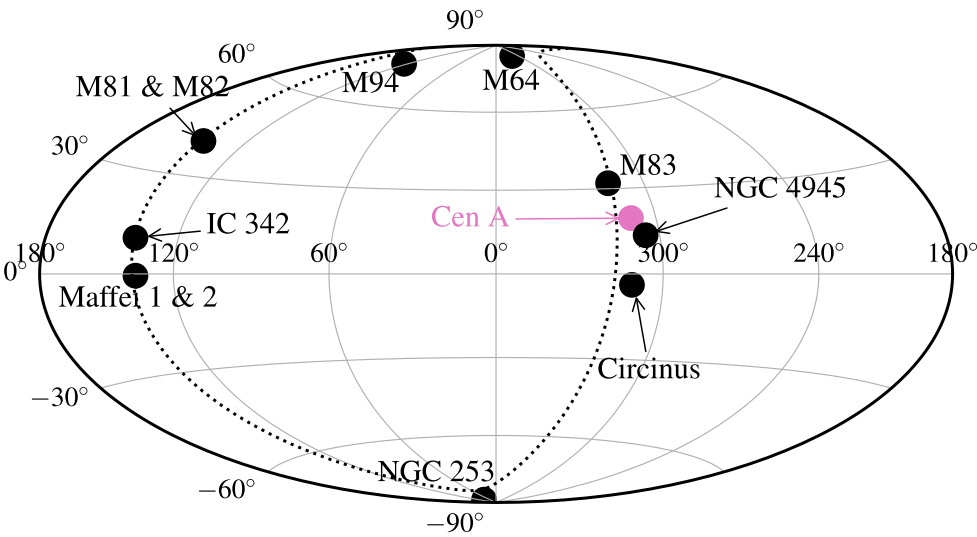


direct 1st echo 2nd echo



Milky Way Based Observations

Green's function solution



Particle Acceleration/Release Scenarios

Model B (source activity):

The UHECR output of Cen A is described by:

$$\mathbf{L} = \mathbf{L}_0 \mathbf{e}^{-\mathbf{t}/\tau_{\text{dec}}}$$

$$\tau_{\text{dec}} = \mathbf{3} \text{ Myr}$$

The UHECR output of Cen A exponentially decays after the initial burst

Model C (leakage):

The UHECR leakage out of Cen A is rigidity dependent

$$\tau_{\text{esc}} = \tau_{10} \left(\frac{(\mathbf{E}/\mathbf{Z})}{\mathbf{10} \text{ EV}} \right)^{-1}$$

$$\tau_{10} = \mathbf{1.5} \text{ Myr}$$

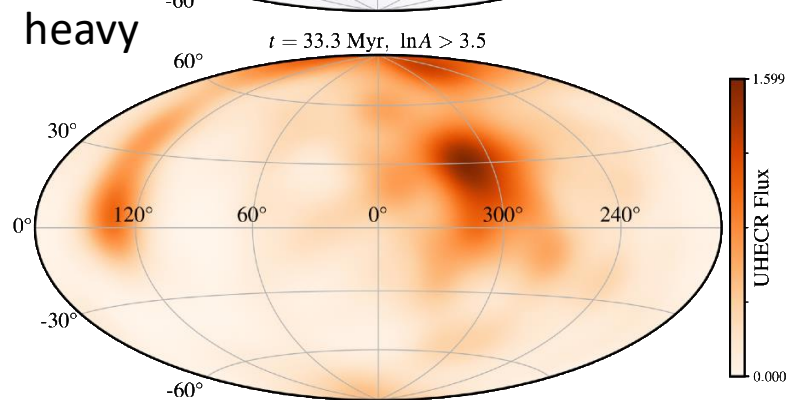
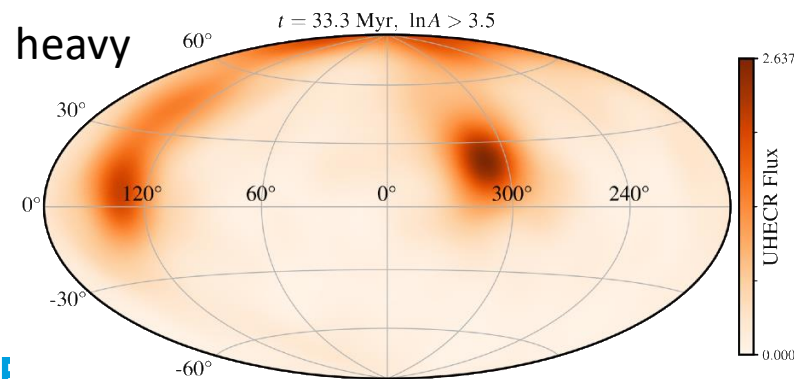
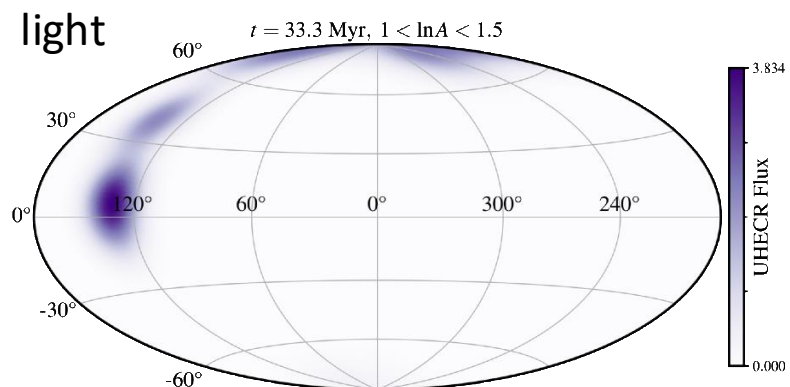
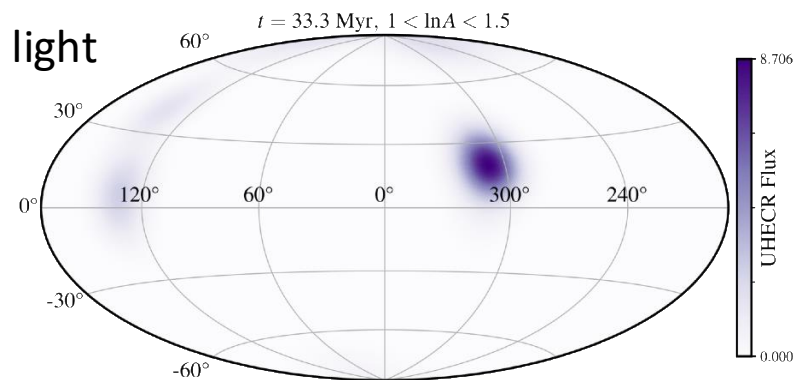
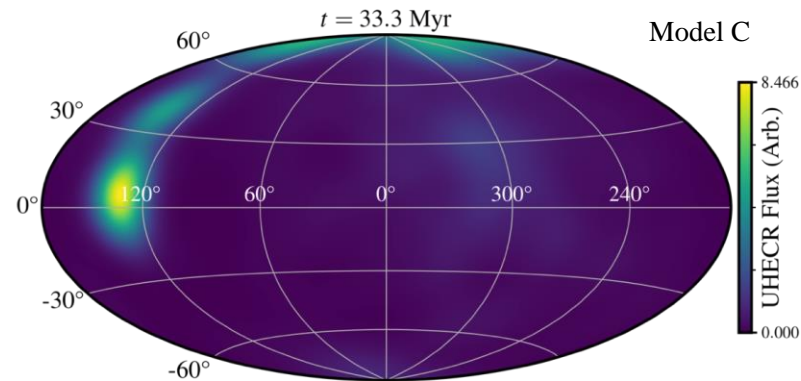
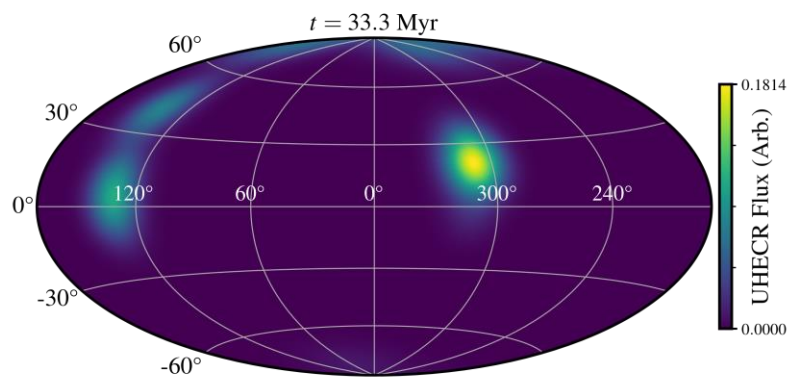
The UHECR were released from the source region in a rigidity dependent manner

Distinguishing Between Model B and Model C Results

Model B (source activity)

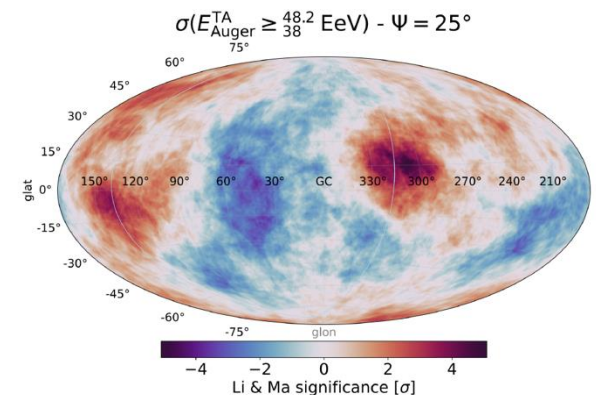
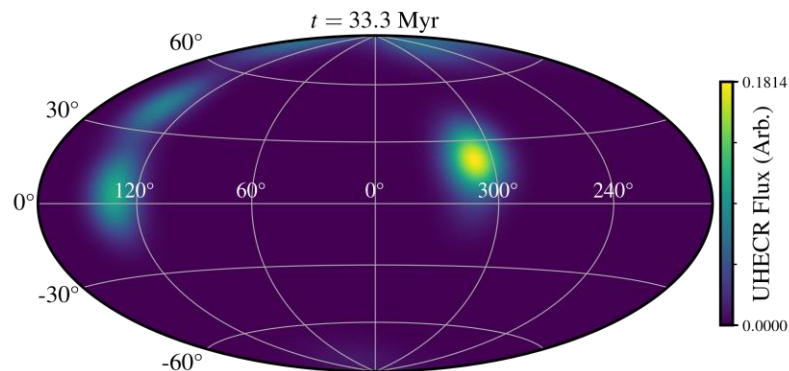
Model C Results

Model C (leakage)



Conclusions

- Cosmic ray data is spectrally consistent with a local source scenario, whose spectral index is consistent with those expectations from Fermi diffusive shock acceleration theory
- Locally (within the Council of Giants) Cen A appears to be the only source capable of accelerating UHECR
- If strong deflections occur in the Council of Giant magnetised halos, this structure can be imprinted onto the arriving UHECR skymap
- Such an imprint may explain the correlation that PAO and TA have reported with local structure
- A key prediction of this scenario is a common composition of the echo regions



Extra Slides

The Uniqueness of Cen A within the Council of Giants

$$t_{\text{acc}} = \eta \frac{R_{\text{lar}}}{c\beta^2}$$

$$t_{\text{esc.}} = \frac{R}{c\beta}$$

[AM Hillas (1984)]

$$E_{\text{max}} = \beta e B R$$

$$L_B = U_B 4\pi R^2 \beta c$$

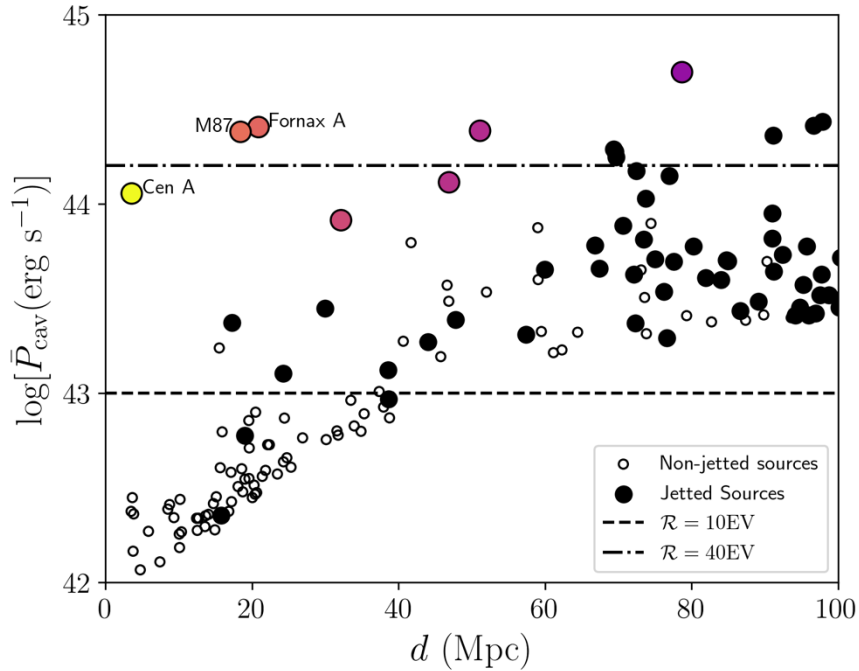
Under the assumption of equipartition of energy between kinetic energy and magnetic field:

[Lovell et al. (1976)]

$$E_{\text{max}} \lesssim \frac{Z}{\eta} (\beta L_{\text{KE}} \alpha \hbar)^{1/2} \approx 10 \frac{Z}{\eta} \left(\frac{\beta L_{\text{KE}}}{3 \times 10^{43} \text{ erg s}^{-1}} \right)^{1/2} \text{ EeV}$$

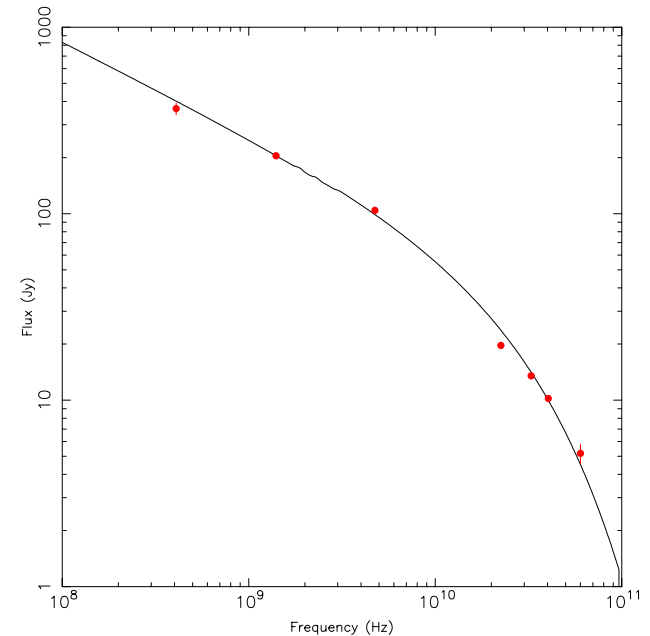
Cen A's Past Activity

Matthews et al. MNRAS 479 (2018)



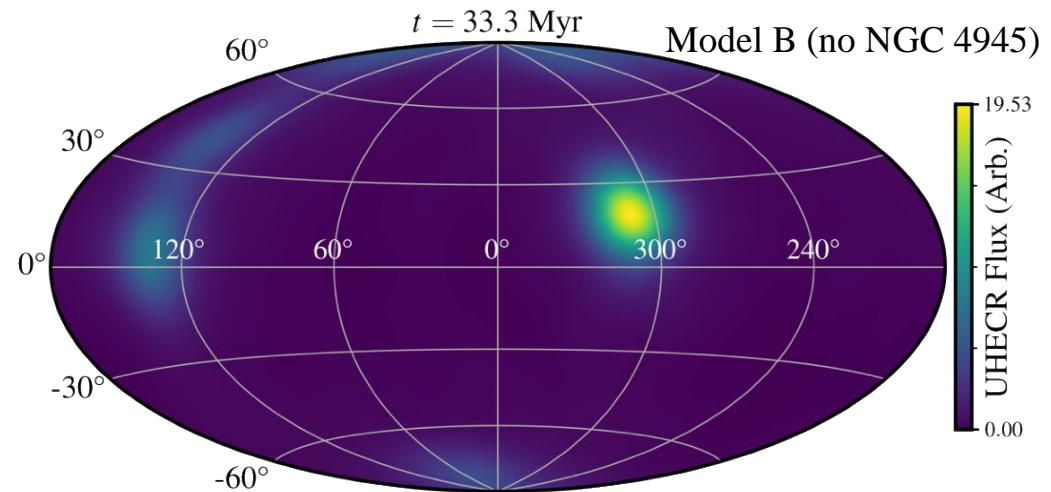
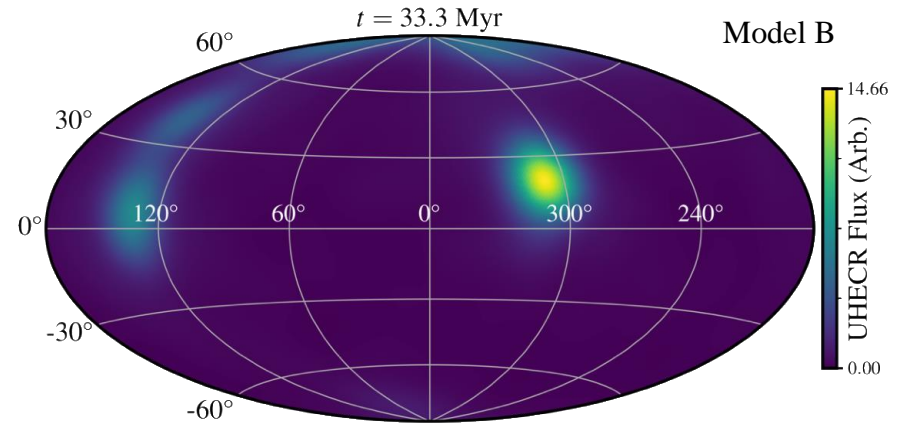
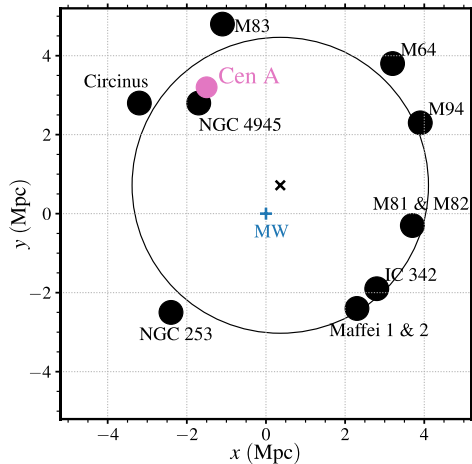
$$L_{\text{jet}} \sim 10^{44} \text{ erg s}^{-1}$$

Hardcastle et al. MNRAS 393 (2009)



$$t_{\text{act}} \sim 20 - 30 \text{ Myrs}$$

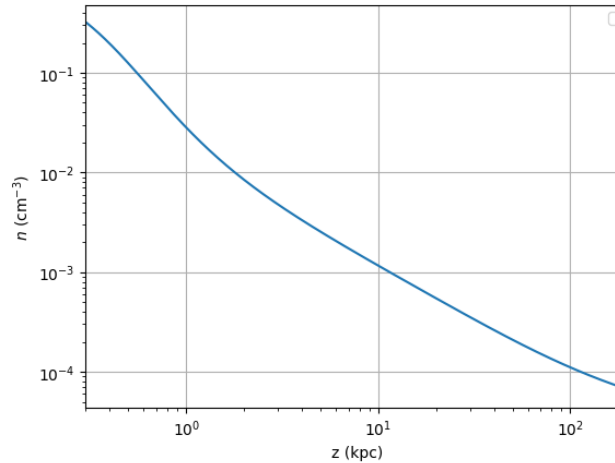
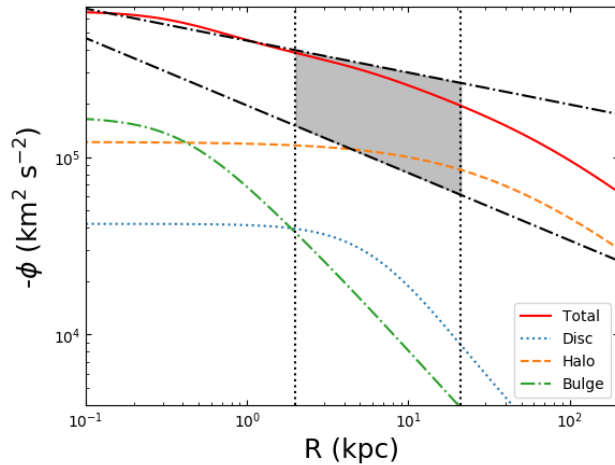
The Presence of NGC 253 in the Skymaps?



Galactic Halo B-field Inference

These results are consistent with expectations if the halo gas is in hydrostatic equilibrium

Faerman ApJ 835 (2017), Tourmente 2207.09189, (2022)



Faerman ApJ, 893 (2020)

$$B(100 \text{ kpc}) \approx 0.2 \mu\text{G}$$



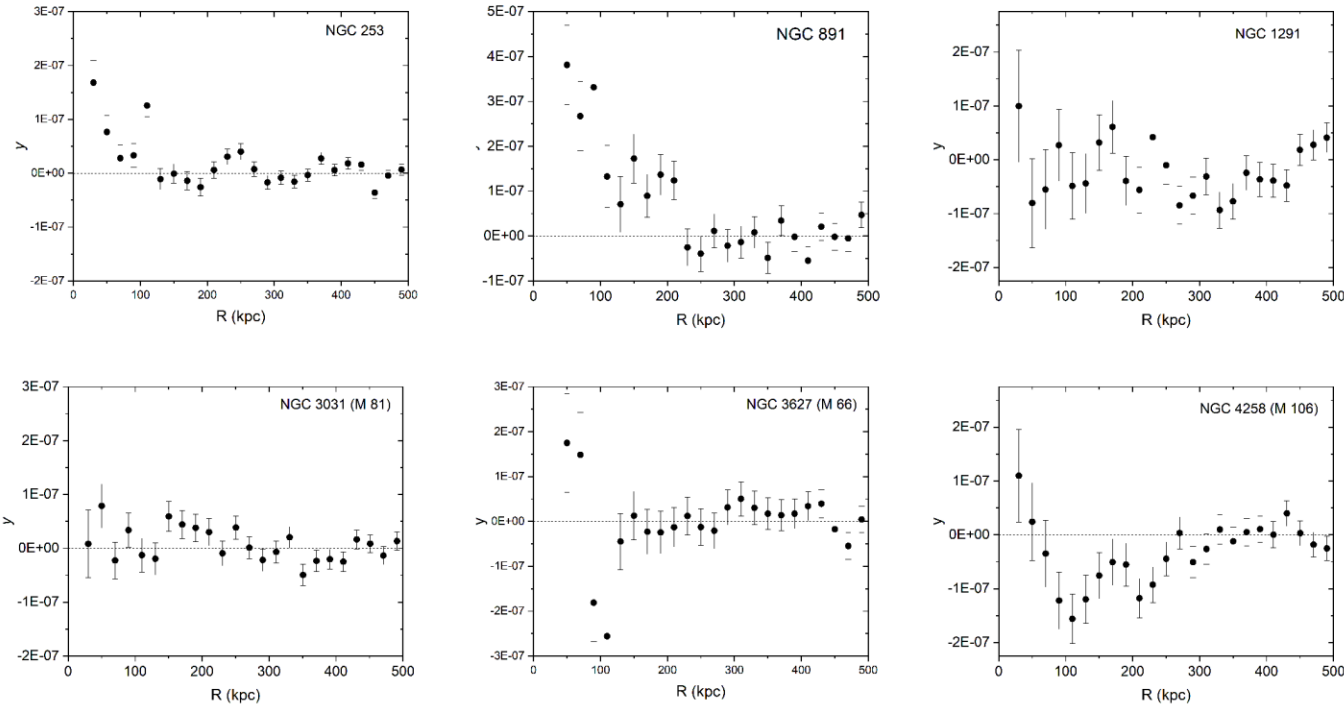
$$r_L(10 \text{ EV}) = 50 \text{ kpc}$$

consistent with

Heesen A&A, 670 (2023)

Extended Hot Gas Around CoG Members?

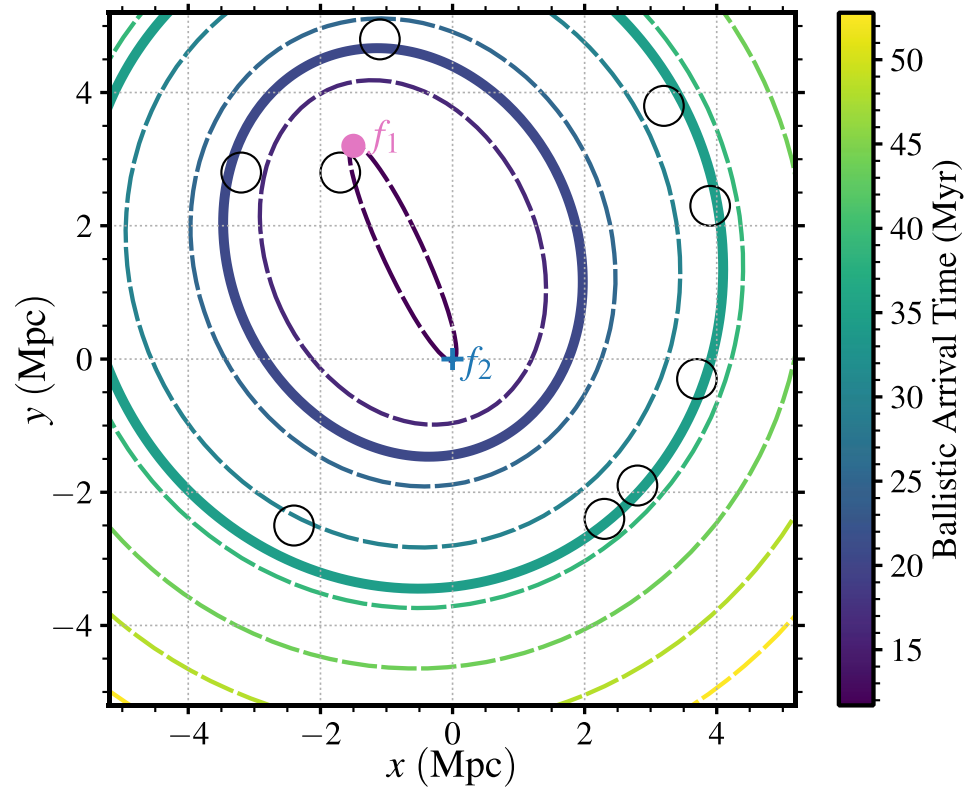
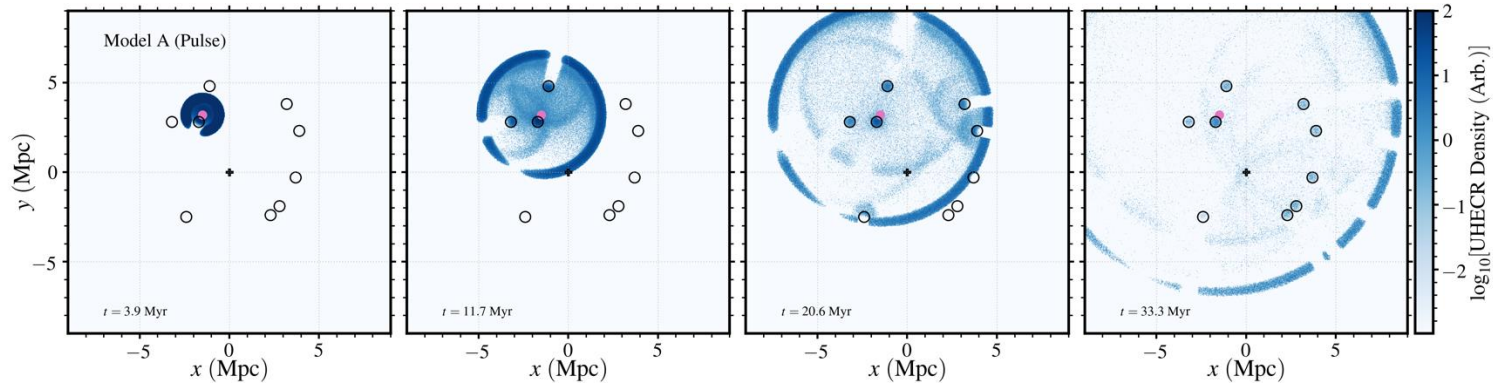
Bregman et al. ApJ 928 (2022)



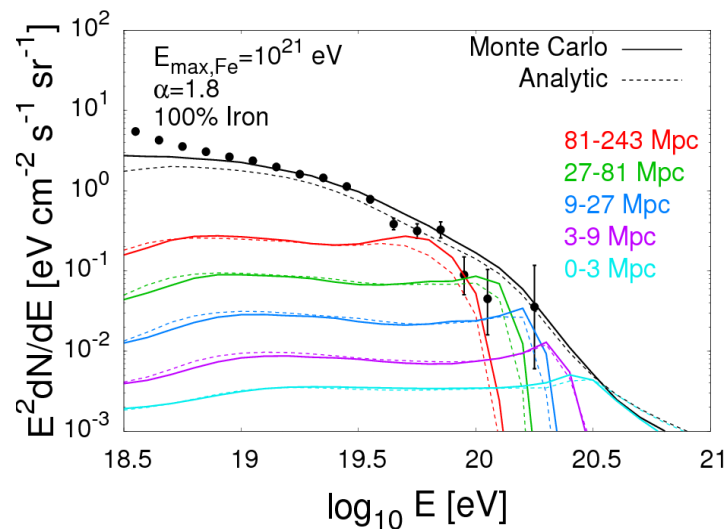
Starburst Activity from CoG Members

Galaxy	l ($^{\circ}$)	b ($^{\circ}$)	Distance (Mpc)	M_* ($10^{10} M_{\odot}$)	$L_{12\mu\text{m}}$ ($10^9 L_{\odot}$)	est. SFR ($M_{\odot} \text{ yr}^{-1}$)
NGC 253	97.36	-87.96	3.5	1.7	3.5	5.4
M64	315.68	84.42	5.0	11.5	1.3	2.3
M81	142.09	40.91	3.7	7.1	0.4	0.8
M82	141.41	40.57	3.5	1.3	7.8	10.7
M83	314.58	31.97	4.9	2.7	3.4	5.2
M94	123.36	76.01	4.5	3.8	0.9	1.6
NGC 4945	305.27	13.34	3.3	1.2	1.8	3.0
IC 342	138.17	10.58	3.4	2.7	2.1	3.5
Maffei 1	135.86	-0.55	3.3	6.2	-	-
Maffei 2	136.50	-0.33	3.4	1.2	0.9	1.5
Circinus	311.33	-3.81	4.3	1.5	6.2	8.8

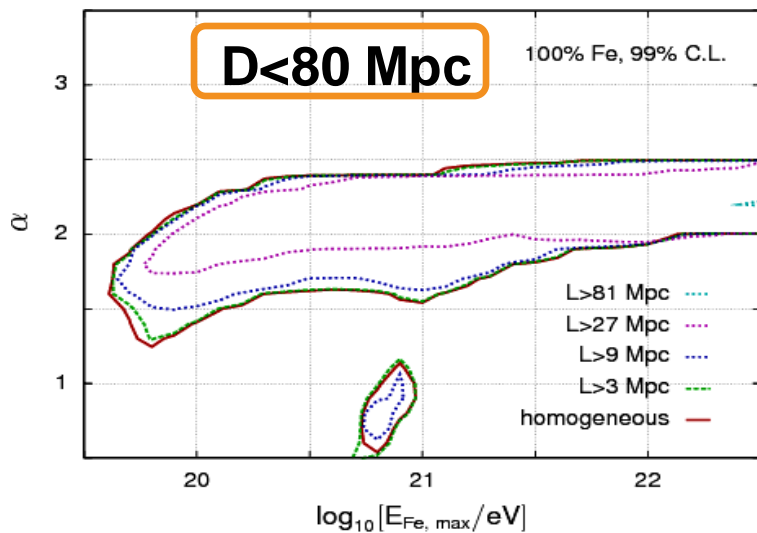
Simulations of UHECR Propagation Through the CoG Structure



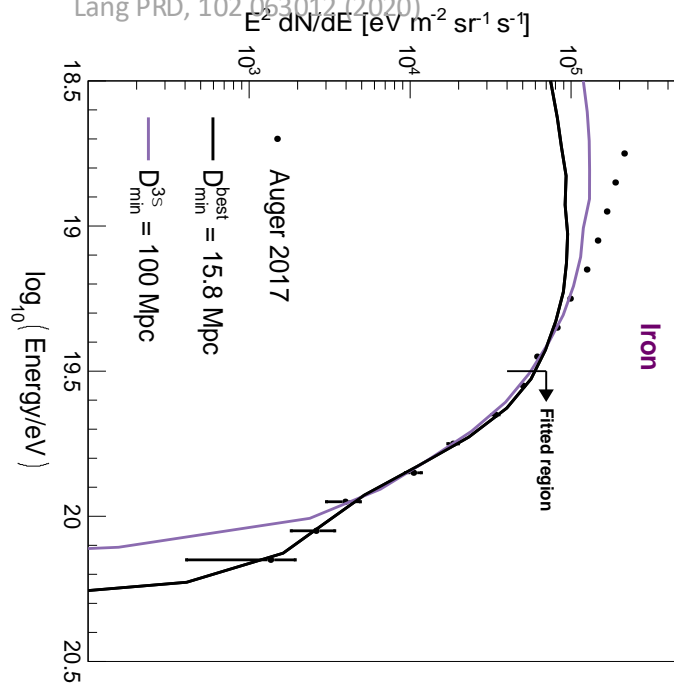
How Far is the Nearest Source?



Taylor PRD, 84 105007 (2011)



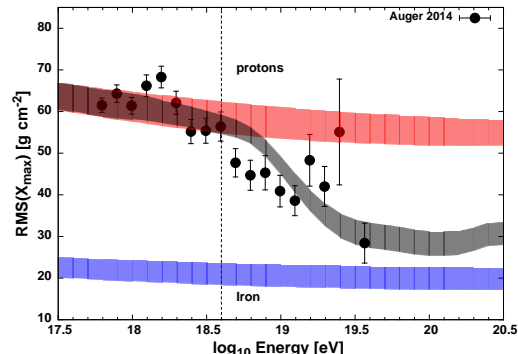
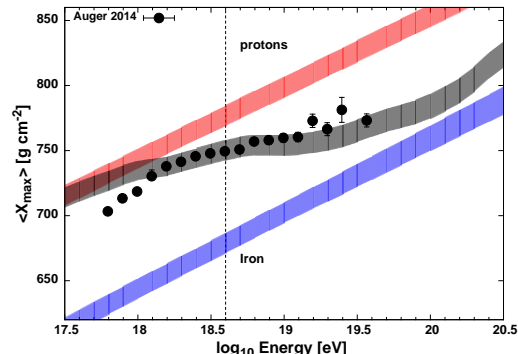
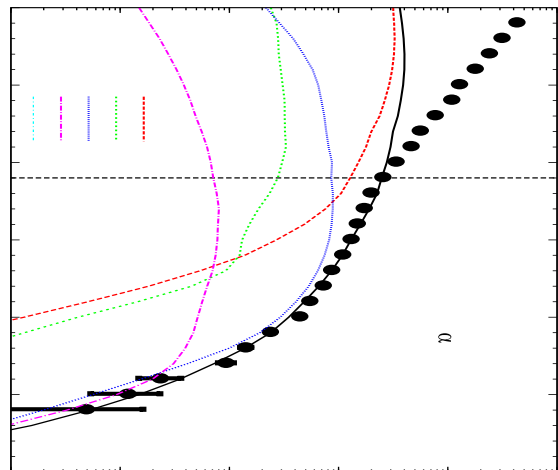
Lang PRD, 102 063012 (2020)



Good Fit Solutions and their Stability

Focusing first on the **spectrum** and **composition** data

Taylor, PRD 92 (2015) 6



Evidence that either there aren't many such sources, or that these sources (spectrally) are copies of each other (ie. stability of solution issues) Ehlert PRD, 107 103045 (2020)

Proximity-Spectral Index Relation

Taylor, PRD 92 (2015) 6

Parameter	$n = -6$		$n = -3$		$n = 0$		$n = 3$	
	Best-fit Value	Posterior Mean & Standard Deviation	Best-fit Value	Posterior Mean & Standard Deviation	Best-fit Value	Posterior Mean & Standard Deviation	Best-fit Value	Posterior Mean & Standard Deviation
α	1.8	1.83 ± 0.31	1.6	1.67 ± 0.36	1.1	1.33 ± 0.41	0.6	0.64 ± 0.44
$\log_{10}\left(\frac{E_{\text{Fe,max}}}{\text{eV}}\right)$	20.5	20.55 ± 0.26	20.5	20.52 ± 0.27	20.2	20.38 ± 0.25	20.2	20.16 ± 0.18

note trend in index 

note trend in index 

PAO, JCAP 04 (2017) 038 source evolution		γ	$\log_{10}(R_{\text{cut}}/V)$	D	$D(J)$	$D(X_{\text{max}})$
$m = +3$		$-1.40^{+0.35}_{-0.09}$	$18.22^{+0.05}_{-0.02}$	179.1	7.5	171.7
$m = 0$		$+0.96^{+0.08}_{-0.13}$	$18.68^{+0.02}_{-0.04}$	174.3	13.2	161.1
$(1+z)^m$	$m = -3$	$+1.42^{+0.06}_{-0.07}$	$18.85^{+0.04}_{-0.07}$	173.9	19.3	154.6
	$m = -6$	$+1.56^{+0.06}_{-0.07}$	18.74 ± 0.03	182.4	19.1	163.3
	$m = -12$	$+1.79 \pm 0.06$	18.73 ± 0.03	182.1	18.1	164.0
	$z \leq 0.02$	$+2.69 \pm 0.01$	$19.50^{+0.08}_{-0.07}$	178.6	15.3	163.3

Local source solution calls upon a more acceptable spectral index

Assumptions on Source Population

$$\frac{dN}{dV_C} \propto (1+z)^n$$

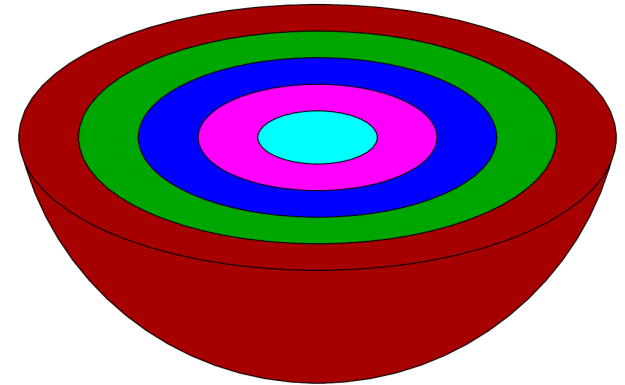
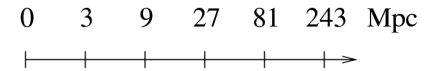
$$z < z_{\max}$$

$$n = -6, -3, 0, 3$$

$$\frac{dN}{dE} \propto \sum_a f_a E^{-\alpha} e^{[-E/E_{Z_a, \max}]}$$

$$E_{Z, \max} = (Z/26) \times E_{Fe, \max}$$

Note- magnetic field horizon effects are neglected in the following. This amounts to assuming: $d_s < (ct_H \lambda_{\text{scat}})^{1/2}$
 ie. the source distribution may be approximated to be spatially continuous (also note, presence of t_H term comes from temporally continuous assumption)



Proximity-Spectral Index Relation

Taylor, PRD 92 (2015) 6

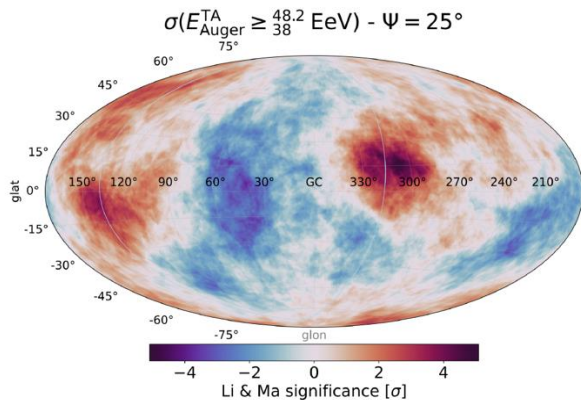
Parameter	$n = -6$		$n = -3$		$n = 0$		$n = 3$	
	Best-fit Value	Posterior Mean & Standard Deviation	Best-fit Value	Posterior Mean & Standard Deviation	Best-fit Value	Posterior Mean & Standard Deviation	Best-fit Value	Posterior Mean & Standard Deviation
α	1.8	1.83 ± 0.31	1.6	1.67 ± 0.36	1.1	1.33 ± 0.41	0.6	0.64 ± 0.44
$\log_{10}\left(\frac{E_{Fe,max}}{eV}\right)$	20.5	20.55 ± 0.26	20.5	20.52 ± 0.27	20.2	20.38 ± 0.25	20.2	20.16 ± 0.18

note trend in index

note trend in index

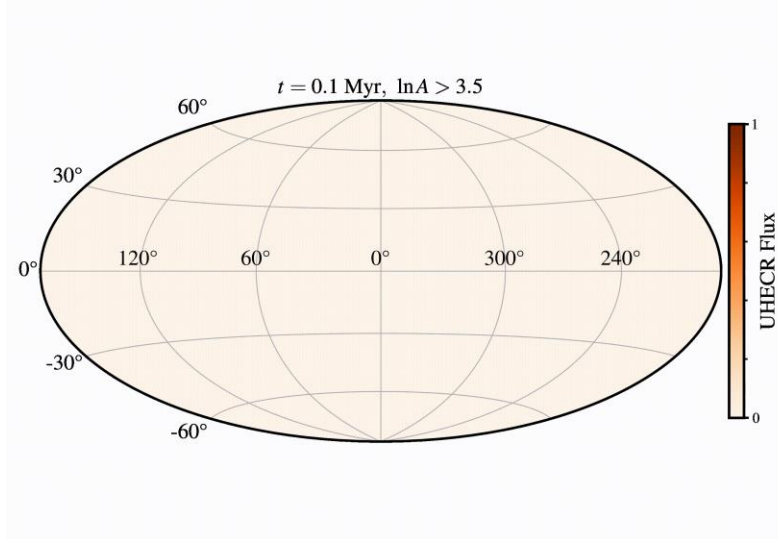
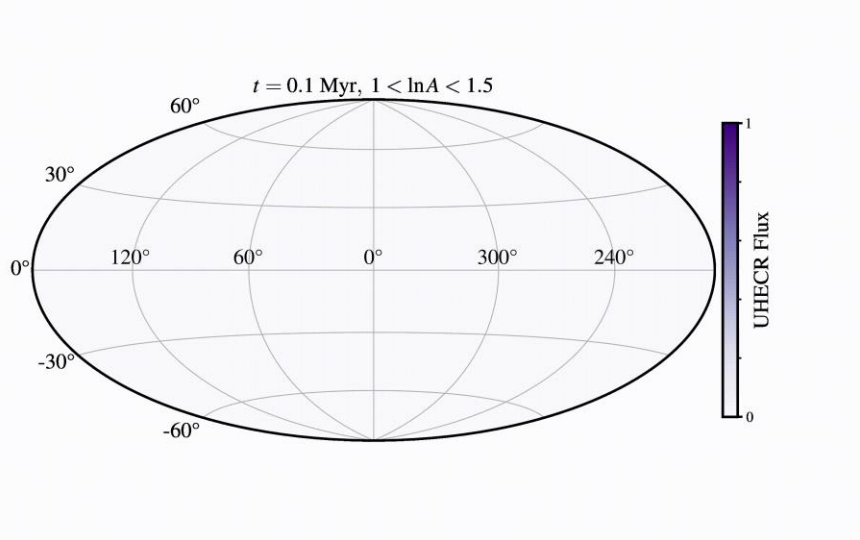
PAO, JCAP 04 (2017) 038
source evolution

	γ	$\log_{10}(R_{cut}/V)$	D	$D(J)$	$D(X_{max})$
$m = +3$	$-1.40^{+0.35}_{-0.09}$	$18.22^{+0.05}_{-0.02}$	179.1	7.5	171.7
$m = 0$	$+0.96^{+0.08}_{-0.13}$	$18.68^{+0.02}_{-0.04}$	174.3	13.2	161.1
$(1+z)^m$ $m = -3$	$+1.42^{+0.06}_{-0.07}$	$18.85^{+0.04}_{-0.07}$	173.9	19.3	154.6
$m = -6$	$+1.56^{+0.06}_{-0.07}$	18.74 ± 0.03	182.4	19.1	163.3
$m = -12$	$+1.79 \pm 0.06$	18.73 ± 0.03	182.1	18.1	164.0
$z \leq 0.02$	$+2.69 \pm 0.01$	$19.50^{+0.08}_{-0.07}$	178.6	15.3	163.3



Local source solution calls upon a more acceptable spectral index- how to square this with the **anisotropy** data?

Model B (source activity)



Model C (leakage)

